Optimal Time-Hopping Codes for Multi-User Interference Mitigation in Ultra-Wide Bandwidth Impulse Radio

Christophe J. Le Martret, Anne-Laure Deleuze, and Philippe Ciblat

***Abstract*— In this work we tackle the problem of mitigating the multi-user interference by optimizing the time-hopping codes, in an asynchronous impulse radio multiple access scheme. We derive the expression of the multi-user interference variance at the output of a rake receiver assuming that the codes are deterministic, for both pulse position modulation and pulse amplitude modulation formats, when propagating through multipath channels. The result shows that the code contribution is independent of the other parameters. We derive from this expression a practical criterion that enables us to find a set of optimal codes that ensures minimal multi-user interference variance at the receiver output. We check through simulations, that the set of optimal codes found using the criterion, leads to bit error rate improvement.**

***Index Terms*— Impulse radio, multiple access, ultra-wideband systems, time-hopping codes, multi-user interference, multipath fading channels.**

I. Introduction

ULTRA Wideband (UWB) communication systems have known a growing interest for the last decade since the first publications on Impulse Radio (IR) [1], [2]. Recently, the Federal Communications Commission (FCC) authorized the use of UWB communication systems in the frequency band from 3.1 GHz to 10.6 GHz [3], but does not specify any modulation format. This event has been followed up by formation of the IEEE Task Group 3a (TG3a) in order to define a new Wireless Personal Area Network (WPAN) standard (IEEE 802.15.3a) based on an UWB physical layer [4]. In this paper, we focus on asynchronous Time-Hopping Codes (THC) Impulse Radio Multiple Access (IRMA), demodulated by a rake receiver as described, for instance, in [2]. In synchronous (or quasi-synchronous) links, the multi-user interference (MUI) may be canceled by the use of orthogonal codes (see *e.g.,* [5] for application to UWB communication systems). Conversely, in asynchronous transmissions, the MUI cannot be nulled and gives rise to Bit Error Rate (BER) floor which limits the system performance. Different works have tackled the characterization of the MUI in order to predict the performance of the system. Many of them have modeled the MUI as a random Gaussian process either in free-space propagation (see *e.g.* [2]), or in multipath channels [6]. Due to their assumptions, the resulting MUI does not depend on the code realization and thus no code optimization is possible. Based upon more general assumptions, and assuming the codes as deterministic, we show that the MUI variance involves the THC values. Thus, this gives a way to mitigate the effect of the MUI by selecting the codes carefully. The criterion we propose here is to select the codes that minimize the variance of the MUI. This is achieved by deriving its exact expression as a function of the code values, and shows explicitly the code contribution to the variance. This derivation is possible thanks to the Developed Time-Hopping Codes (DTHC), originally introduced in [5]. This result is established for a very generic channel that encompasses most of the conventional models for UWB. It is valid for Pulse Position Modulation (PPM) format as well as for Pulse Amplitude Modulation (PAM) and is independent of the number of fingers of the rake receiver. Although the Gaussian approximation is not valid for performance evaluation [9], one can imagine that minimizing the variance of the MUI should lead to performance improvement. We verify through simulations, that the optimal code leads to increasing the performance in terms of BER.

The document is organized as follows. In Section II we introduce the notations, give the transmitted signal model both for PPM and PAM formats, the channel model and the rake receiver structure. In Section III, we derive the variance expression of the MUI for the PPM and the PAM formats. The results show the explicit relationship between the user codes and the variance. In Section IV, we establish some properties of the DTHC and deduce the criterion enabling the choice of codes which minimize the MUI variance. In Section V we illustrate our results by simulations, showing that the signal to noise ratio (SNR) criterion translates into BER performance improvement, which validates our code optimization process. We conclude in Section VI.

Manuscript received July 10, 2004; revised December 15, 2004 and March 7, 2005; accepted March 12, 2005. The associate editor coordinating the review of this paper and approving it for publication was Z. Tian. Part of the results have been presented to the Asilomar Conference on Signals, Systems and Computers, November 2004.

Christophe J. Le Martret and Anne-Laure Deleuze are with THALES Land and Joint Systems, 160 Boulevard de Valmy, B.P. 82, 92704 Colombes Cedex, France (e-mail: christophe.le_martret@fr.thalesgroup.com; anne-laure.deleuze@fr.thalesgroup.com).

Philippe Ciblat is with the Département Communications et Électronique, École Nationale Supérieure des Télécommunications (ENST), 46 rue Barrault, 75013 Paris, France (e-mail: philippe.ciblat@enst.fr).

Digital Object Identifier 10.1109/TWC.2006.04446

II. Signal Model

A. Transmitted Signals

The UWB signals we are considering in this paper are TH-IRMA with PPM and PAM formats. The modulations will

be considered binary for the sake of presentation clarity, but results can be easily extended to higher-order modulations.

PPM Format: The PPM signal transmitted by user n is given by:

$$s_n(t) = \sum_{i=-\infty}^{+\infty} w(t - iT_f - \tilde{c}_n(i)T_c - \delta d_n(\lfloor i/N_f \rfloor) - \theta_n), \quad (1)$$

where N_f is the number of frames of duration $T_f := N_c T_c$ with N_c the number of chips of duration T_c, $w(t)$ is the impulse of duration $T_w \ll T_c$, $\delta \ll T_c$ is the PPM shift, $\lfloor x \rfloor$ denotes the integer-floor of x, and $d_n(i) \in \{0, 1\}$ are the transmitted symbols assumed to be independent and identically distributed. Thus, a symbol is repeated N_f times with one pulse in each frame. The THC sequence $\{\tilde{c}_n(i)\}$ values are drawn in $[0, N_c - 1]$[1] and are assumed to be periodic of period $P_{\tilde{c}} := N_f$. The variable θ_n accounts for the asynchronism between the different users and will be modeled as uniformly distributed over a code period $[0, N_f T_f)$. With this assumption, expression (1) can be re-expressed as:

$$s_n(t) = \sum_{i=-\infty}^{+\infty} b_n(t - iN_f T_f - \delta d_n(i) - \theta_n), \quad (2)$$

$$b_n(t) = \sum_{j=0}^{N_f - 1} w(t - jT_f - \tilde{c}_n(j)T_c). \quad (3)$$

Moreover, it is instrumental to re-express (3) using the so-called *developed time-hopping codes* [5]. The basic idea of the DTHC is to take out the code contribution from the argument of the pulse, and to put it as a factor. The transmitted signal can be thus expressed as a kind of On-Off Keying modulation at symbol rate T_c by modulating the pulse with a one when $iT_f - \tilde{c}_n(i)T_c = 0$ and with zero otherwise. Thus, (3) can be re-written in an equivalent way by:

$$b_n(t) = \sum_{j=0}^{N_c N_f - 1} c_n(j) w(t - jT_c), \quad (4)$$

where the DTHC sequence $c_n := \{c_n(j)\}_{j=0}^{N_c N_f - 1}$ is deduced from sequence $\{\tilde{c}_n(i)\}_{i=0}^{N_f - 1}$ by:

$$c_n(j) = \begin{cases} 1 & \text{if } j = \tilde{c}_n(i) + iN_c,\ 0 \le i \le N_f - 1, \\ 0 & \text{otherwise.} \end{cases} \quad (5)$$

As a consequence, DTHC are periodic with period $P_c := N_c P_{\tilde{c}}$. Finally, combining (2) and (4), leads to the following expression:

$$s_n(t) = \sum_{i=-\infty}^{+\infty} \sum_{j=0}^{N_c N_f - 1} c_n(j) w(t - iN_f T_f - jT_c - \delta d_n(i) - \theta_n). \quad (6)$$

PAM Format: The expression of a THC-IR signal with the PAM format, using the DTHC, is given by:

$$s_n(t) = \sum_{i=-\infty}^{+\infty} d_n(i) \sum_{j=0}^{N_c N_f - 1} c_n(j) w(t - iN_f T_f - jT_c - \theta_n), \quad (7)$$

where the symbols $d_n(i)$ belong to the set $\{-1, +1\}$.

[1]This model encompasses as well the case where $T_f < N_c T_c$, in order to account for guard time, by restricting the maximum range of the code values. For more details, see [5].

B. Channel Model

In order to present results as general as possible, we will consider a specular channel that encompasses most of the models proposed so far. The channel impulse response between user n and the receiver is given by $h_n(t) = \sum_{k=1}^{N_p} A_n^k \delta(t - \tau_n^k)$, where N_p is the number of paths, A_n^k and τ_n^k are respectively the amplitude and the delay of the k-th path. We assume that the delays verify $\forall n, k,\ \tau_n^k < \tau_n^{k+1}$. For simplicity, we will assume that the number of paths is the same for all the users, but generalization to a different number of paths per user is straightforward. In many multipath channel models, the amplitudes A_n^k depend on the corresponding delays τ_n^k. We propose to model this dependency by setting $A_n^k = a_n^k \cdot f(\tau_n^k)$ where a_n^k is a random variables (*rv*) that accounts for the statistics of the amplitude (independent of τ_n^k) and $f(\cdot)$ is a function that accounts for the decaying of the amplitude with respect to the delay. The *rv* a_n^k are assumed to be independent and zero mean with variance $\sigma_a^2 := \mathbb{E}_a[(a_n^k)^2]$ and thus verify $\mathbb{E}_a(a_{n_1}^{k_1} a_{n_2}^{k_2}) = \mathbb{E}_a(a_{n_1}^{k_1})\mathbb{E}_a(a_{n_2}^{k_2}) = 0$, except for the case $k_1 = k_2$ and $n_1 = n_2$. In the following we put $I_n^k := \mathbb{E}_a[(A_n^k)^2] = \sigma_a^2 \cdot f^2(\tau_n^k)$. The *rv* τ_n^k are assumed to be independent between users but are usually correlated for a given user. Most of the channel models proposed for the UWB can be cast into this general model, and more particularly, the recent modified Saleh-Valenzuela model, which has been selected in the TG3a for the IEEE 802.15.3a standard [11]. In this model, the arrival time of the ℓ-th cluster T_ℓ and the arrival time of the k-th ray measured from the beginning of the ℓ-th cluster $\tau_{\ell k}$, follow Poisson processes with parameter Λ and λ respectively. The amplitude $a_n^k = p_n^k \cdot \beta_n^k$, where p_n^k is equi-probable ± 1 and β_n^k is a log-normal *rv*. The function $f(\cdot)$ can be identified as: $f(\tau_n^k) = e^{-\tau_n^k / 2\Gamma\gamma}$, where $\{\tau_n^k\}$ is the set of sorted values drawn from the set $\{\gamma T_\ell + \Gamma \tau_{\ell k}\}$. Likewise, for the original Saleh-Valenzuela model [7], the amplitudes a_k^n are real-valued zero mean Gaussian *rv* while $f(\cdot)$ remains the same.

The communication system considered in this paper consists of N_u active users transmitting asynchronously. After propagating, the signal from user n is given by $r_n(t) = \sum_{k=1}^{N_p} A_n^k s_n(t - \tau_n^k)$, and the composite signal seen at a receiver can be expressed as:

$$r(t) := \sum_{n=1}^{N_u} r_n(t) + n(t) \quad (8)$$

where $n(t)$ is the Additive White Gaussian Noise (AWGN) with zero mean and variance $N_0/2$.

C. Rake Receiver

In this study we consider Maximum Ratio Combining (MRC) rake receivers with $L_r \le N_p$ fingers, (A_1^ℓ, τ_1^ℓ), $\ell \in \mathscr{L}$, with $\mathrm{Card}(\mathscr{L}) = L_r$. Depending on the subset $\mathscr{L}$, we classically achieve the classical PRAKE, SRAKE and Full-Rake receivers (see *e.g.*, [12]). In the sequel, we assume that the receiver is synchronized on user 1, and that $\theta_1 = 0$ without loss of generality. The rake output can be written as:

$$z = \sum_{\ell \in \mathscr{L}} A_1^\ell \int_0^{N_f T_f} r(t + \tau_1^\ell) v_1(t) dt, \quad (9)$$

where $v_1(t)$ is the receiver template for user 1, which using the DTHC definition, can be expressed as:

$$v_1(t) := \sum_{j=0}^{N_c N_f - 1} c_1(j) v(t - jT_c), \tag{10}$$

with $v(t) := w(t) - w(t-\delta)$ in the binary PPM case and $v(t) := w(t)$ in the PAM case.

Using (8)-(10), the rake output expression becomes:

$$z = \sum_{\ell \in \mathscr{L}} A_1^\ell \sum_{n=1}^{N_u} \sum_{k=1}^{N_p} A_n^k \, y_{k,\ell,n}(\theta_n) + \eta, \tag{11}$$

where $\eta := \sum_{\ell \in \mathscr{L}} A_1^\ell \int_0^{N_f T_f} n(t + \tau_1^\ell) v_1(t) dt$ is the filtered noise, and in the PPM case:

$$\begin{aligned} y_{k,\ell,n}(\theta_n) := \int_0^{N_f T_f} \sum_{i=-\infty}^{+\infty} \sum_{j=0}^{N_c N_f - 1} c_n(j) \\ w(t - iN_f T_f - jT_c - \delta d_n(i) - \theta_n - \Delta\tau_{k,\ell,n}) \cdot v_1(t) dt, \end{aligned} \tag{12}$$

and in the PAM case:

$$\begin{aligned} y_{k,\ell,n}(\theta_n) := \int_0^{N_f T_f} \sum_{i=-\infty}^{+\infty} d_n(i) \sum_{j=0}^{N_c N_f - 1} c_n(j) \\ w(t - iN_f T_f - jT_c - \theta_n - \Delta\tau_{k,\ell,n}) \cdot v_1(t) dt, \end{aligned} \tag{13}$$

with $\Delta\tau_{k,\ell,n} := \tau_n^k - \tau_1^\ell$. Expression (11) can be separated into four terms

$$z := z_1 + z_2 + z_3 + \eta, \tag{14}$$

with

$$z_1 = \sum_{\ell \in \mathscr{L}} (A_1^\ell)^2 y_{\ell,\ell,1}(0), \quad z_2 = \sum_{\ell \in \mathscr{L}} A_1^\ell \sum_{k \neq \ell = 1}^{N_p} A_1^k y_{k,\ell,1}(0),$$

and

$$z_3 = \sum_{\ell \in \mathscr{L}} A_1^\ell \sum_{n=2}^{N_u} \sum_{k=1}^{N_p} A_n^k y_{k,\ell,n}(\theta_n), \tag{15}$$

which can be interpreted as follow:

- z_1 is the energy collected from the user of interest,
- z_2 is the Inter-Symbol / Inter-Frame Interference (ISI / IFI) for the user of interest,
- z_3 is the multi-user interference.

The energy z_1 and the filtered noise η do not depend on the code selection whereas z_2 and z_3 do. In practical systems the ISI / IFI can be chosen arbitrarily small regardless of the codes by inserting a guard time, larger than the maximum delay spread of the channel, placed at the end of each frame (see *e.g.*, [8]). In contrast, the MUI is inherent in the THC-IR transmission scheme and can be mitigated only by designing the codes properly. Therefore, as mentioned in the introduction, the rest of the paper will be dedicated to the research of optimal codes that minimize the MUI variance.

III. Variance Expression of the MUI

A. Variance of z_3 in the PPM Case

Since the random variables involved in z_3 are assumed independent, we can compute the expectation independently one after another. For convenience purpose, we present the computation taking the expectation in the following order: a_n^k, d_n, θ_n and τ_n^k. It is easy to verify that z_3 is centered since the amplitudes are centered. Thus, based on expression (37) of $y_{k,\ell,n}(\theta_n)$ derived in the Appendix, the expectation of z_3^2 over the amplitude, is given by:

$$\begin{aligned} \mathbb{E}_a(z_3^2) &= \sum_{n,k,\ell} I_n^k I_1^\ell \big[\mathscr{C}_{1,n}^{-2}(q_n^{k,\ell}) \rho_{\varepsilon_n^{k,\ell}, \varepsilon_n^{k,\ell}}^{-Q_n^{k,\ell}-1, -Q_n^{k,\ell}-1} \\ &+ \mathscr{C}_{1,n}^{-2}(q_n^{k,\ell}+1) \rho_{\varepsilon_n^{k,\ell}-T_c, \varepsilon_n^{k,\ell}-T_c}^{-Q_n^{k,\ell}-1, -Q_n^{k,\ell}-1} \\ &+ \mathscr{C}_{1,n}^{+2}(q_n^{k,\ell}) \rho_{\varepsilon_n^{k,\ell}, \varepsilon_n^{k,\ell}}^{-Q_n^{k,\ell}, -Q_n^{k,\ell}} \\ &+ \mathscr{C}_{1,n}^{+2}(q_n^{k,\ell}+1) \rho_{\varepsilon_n^{k,\ell}-T_c, \varepsilon_n^{k,\ell}-T_c}^{-Q_n^{k,\ell}, -Q_n^{k,\ell}} \\ &+ 2\mathscr{C}_{1,n}^{-}(q_n^{k,\ell}) \mathscr{C}_{1,n}^{+}(q_n^{k,\ell}) \rho_{\varepsilon_n^{k,\ell}, \varepsilon_n^{k,\ell}}^{-Q_n^{k,\ell}-1, -Q_n^{k,\ell}} \\ &+ 2\mathscr{C}_{1,n}^{-}(q_n^{k,\ell}+1) \mathscr{C}_{1,n}^{+}(q_n^{k,\ell}+1) \, \rho_{\varepsilon_n^{k,\ell}-T_c, \varepsilon_n^{k,\ell}-T_c}^{-Q_n^{k,\ell}-1, -Q_n^{k,\ell}} \big], \end{aligned} \tag{16}$$

where $\rho_{i_1,i_2}^{p_1,p_2} := r_{vw}(i_1 + \delta d_n(p_1)) r_{vw}(i_2 + \delta d_n(p_2))$ and the bounds for variables n, k, ℓ are omitted for simplicity, but follow the one indicated in (15). Because the time support of $r_{vw}(\cdot)$ is much less than T_c, $\rho_{\varepsilon_n^{k,\ell}, \varepsilon_n^{k,\ell}-T_c}^{p_1,p_2} = 0$, $\forall p_1, p_2$. The expressions of $\mathscr{C}_{1,n}^{-}(j)$ and $\mathscr{C}_{1,n}^{+}(j)$ are provided in (34) and (36) respectively.

The expectation of (16) over the symbols brings the following terms to be calculated: $\mathbb{E}_d(\rho_{j,j}^{i,i})$, $\mathbb{E}_d(\rho_{j,j}^{i-1,i-1})$, and $\mathbb{E}_d(\rho_{j,j}^{i,i-1})$.

Basic computation gives:

$$\begin{aligned} \mathbb{E}_d(\rho_{j,j}^{i,i}) &= \mathbb{E}_d(\rho_{j,j}^{i-1,i-1}) = \frac{1}{2} r_{vw}^2(j) + \frac{1}{2} r_{vw}^2(j+\delta), \\ \mathbb{E}_d(\rho_{j,j}^{i,i-1}) &= \frac{1}{4} \big[r_{vw}(j) + r_{vw}(j+\delta) \big]^2. \end{aligned}$$

Thus, we finally obtain:

$$\begin{aligned} \mathbb{E}_{a,d}(z_3^2) = \frac{1}{2} \sum_{n,k,\ell} I_n^k I_1^\ell \big[\big[\mathscr{C}_{1,n}^{+2}(q_n^{k,\ell}) + \mathscr{C}_{1,n}^{-2}(q_n^{k,\ell}) \big] \\ \times \big[r_{vw}^2(\varepsilon_n^{k,\ell}) + r_{vw}^2(\varepsilon_n^{k,\ell} + \delta) \big] \\ + \big[\mathscr{C}_{1,n}^{+2}(q_n^{k,\ell}+1) + \mathscr{C}_{1,n}^{-2}(q_n^{k,\ell}+1) \big] \\ \times \big[r_{vw}^2(\varepsilon_n^{k,\ell} - T_c) + r_{vw}^2(\varepsilon_n^{k,\ell} - T_c + \delta) \big] \\ + \mathscr{C}_{1,n}^{+}(q_n^{k,\ell}) \mathscr{C}_{1,n}^{-}(q_n^{k,\ell}) \big[r_{vw}(\varepsilon_n^{k,\ell}) + r_{vw}(\varepsilon_n^{k,\ell} + \delta) \big]^2 \\ + \mathscr{C}_{1,n}^{+}(q_n^{k,\ell}+1) \mathscr{C}_{1,n}^{-}(q_n^{k,\ell}+1) \\ \times \big[r_{vw}(\varepsilon_n^{k,\ell} - T_c) + r_{vw}(\varepsilon_n^{k,\ell} + \delta - T_c) \big]^2 \big]. \end{aligned}$$

In the sequel, we average $\mathbb{E}_{a,d}(z_3^2)$ over θ_n assuming $\Delta\tau_{k,\ell,n}$ fixed. Since θ_n is uniformly distributed over

$[0, N_f T_f)$, we get

$$\begin{aligned}\mathbb{E}_{a,d,\theta}(z_3^2) = \frac{1}{2N_f T_f} \sum_{n,k,\ell} I_n^k I_1^\ell \int_0^{N_f T_f} \Big[& \\ & \big[\mathscr{C}_{1,n}^{+2}(q_n^{k,\ell}) + \mathscr{C}_{1,n}^{-2}(q_n^{k,\ell})\big] \\ & \times \big[r_{vw}^2(\varepsilon_n^{k,\ell}) + r_{vw}^2(\varepsilon_n^{k,\ell} + \delta)\big] \\ & + \big[\mathscr{C}_{1,n}^{+2}(q_n^{k,\ell}+1) + \mathscr{C}_{1,n}^{-2}(q_n^{k,\ell}+1)\big] \\ & \times \big[r_{vw}^2(\varepsilon_n^{k,\ell} - T_c) + r_{vw}^2(\varepsilon_n^{k,\ell} - T_c + \delta)\big] \\ & + \mathscr{C}_{1,n}^{+}(q_n^{k,\ell})\mathscr{C}_{1,n}^{-}(q_n^{k,\ell})\big[r_{vw}(\varepsilon_n^{k,\ell}) + r_{vw}(\varepsilon_n^{k,\ell} + \delta)\big]^2 \\ & + \mathscr{C}_{1,n}^{+}(q_n^{k,\ell}+1)\mathscr{C}_{1,n}^{-}(q_n^{k,\ell}+1) \\ & \times \big[r_{vw}(\varepsilon_n^{k,\ell} - T_c) + r_{vw}(\varepsilon_n^{k,\ell} + \delta - T_c)\big]^2\Big] d\theta_n.\end{aligned}$$

Notice that $q_n^{k,\ell}$ and $\varepsilon_n^{k,\ell}$ depend on θ_n via (31). To simplify the previous equation, we split the integral of the right hand side of the previous equation into $N_c N_f$ integrals over the interval $[0, T_c)$. After tedious computation, we find:

$$\begin{aligned}\mathbb{E}_{a,d,\theta}(z_3^2) = \frac{1}{2N_f T_f} \sum_{n,k,\ell} I_n^k I_1^\ell \sum_{q=0}^{N_c N_f - 1} \int_0^{T_c} \Big[& \\ & \big[\mathscr{C}_{1,n}^{+2}(q) + \mathscr{C}_{1,n}^{-2}(q)\big] \\ & \times \big[r_{vw}^2(\varepsilon) + r_{vw}^2(\varepsilon + \delta)\big] \\ & + \big[\mathscr{C}_{1,n}^{+2}(q+1) + \mathscr{C}_{1,n}^{-2}(q+1)\big] \\ & \times \big[r_{vw}^2(\varepsilon - T_c) + r_{vw}^2(\varepsilon - T_c + \delta)\big] \\ & + \mathscr{C}_{1,n}^{+}(q)\mathscr{C}_{1,n}^{-}(q)\big[r_{vw}(\varepsilon) + r_{vw}(\varepsilon + \delta)\big]^2 \\ & + \mathscr{C}_{1,n}^{+}(q+1)\mathscr{C}_{1,n}^{-}(q+1) \\ & \times \big[r_{vw}(\varepsilon - T_c) + r_{vw}(\varepsilon + \delta - T_c)\big]^2\Big] d\varepsilon. \quad (17)\end{aligned}$$

We can easily show, by the periodicity of the codes, that:

$$\sum_{q=0}^{N_c N_f - 1} \big[\mathscr{C}_{1,n}^{+2}(q+1) + \mathscr{C}_{1,n}^{-2}(q+1)\big] = \sum_{q=0}^{N_c N_f - 1} \big[\mathscr{C}_{1,n}^{+2}(q) + \mathscr{C}_{1,n}^{-2}(q)\big],$$

and

$$\sum_{q=0}^{N_c N_f - 1} \mathscr{C}_{1,n}^{+}(q+1)\mathscr{C}_{1,n}^{-}(q+1) = \sum_{q=0}^{N_c N_f - 1} \mathscr{C}_{1,n}^{+}(q)\mathscr{C}_{1,n}^{-}(q).$$

Thus (17) reduces to:

$$\begin{aligned}\mathbb{E}_{a,d,\theta}(z_3^2) = \frac{1}{2N_f T_f} \sum_{n,k,\ell} \sum_{q=0}^{N_c N_f - 1} I_n^k I_1^\ell \int_0^{T_c} \Big[& \\ & \Big[\mathscr{C}_{1,n}^{+2}(q) + \mathscr{C}_{1,n}^{-2}(q)\Big]\Big[r_{vw}^2(\varepsilon) + r_{vw}^2(\varepsilon + \delta) \\ & + r_{vw}^2(\varepsilon - T_c) + r_{vw}^2(\varepsilon - T_c + \delta)\Big] \\ & + \mathscr{C}_{1,n}^{+}(q)\mathscr{C}_{1,n}^{-}(q)\Big[\big[r_{vw}(\varepsilon) r_{vw}(\varepsilon + \delta)\big]^2 \\ & + \big[r_{vw}(\varepsilon - T_c) + r_{vw}(\varepsilon + \delta - T_c)\big]^2\Big] d\varepsilon. \quad (18)\end{aligned}$$

Finally, we deduce that the expectation over θ_n provides

$$\begin{aligned}\mathbb{E}_{a,d,\theta}(z_3^2) = \frac{1}{N_f T_f} \sum_{\ell \in \mathscr{L}} I_1^\ell \sum_{k=1}^{N_p} \sum_{n=2}^{N_u} I_n^k \sum_{q=0}^{N_c N_f - 1} \Big[& \\ & \big[\mathscr{C}_{1,n}^{+2}(q) + \mathscr{C}_{1,n}^{-2}(q)\big] \cdot \gamma_{vw}(0) \\ & + \mathscr{C}_{1,n}^{+}(q)\mathscr{C}_{1,n}^{-}(q) \cdot \big[\gamma_{vw}(0) + \gamma_{vw}(\delta)\big]\Big], \quad (19)\end{aligned}$$

with $\gamma_{vw}(s) := \int_{-\infty}^{+\infty} r_{vw}(x - s) r_{vw}(x) dx$.

Now we need to average (19) over the delays $\Delta\tau_{k,\ell,n}$. After straightforward manipulations, we obtain that the term $\sigma_3^2 := \mathbb{E}_{a,d,\theta,\tau}(z_3^2)$ writes as follows

$$\sigma_3^2 = \frac{\psi\ \gamma_{vw}(0)}{N_f T_f}\big[\kappa_1 + \bar{\gamma} \cdot \xi_1\big], \quad (20)$$

where

$$\bar{\gamma} := \frac{\gamma_{vw}(0) + \gamma_{vw}(\delta)}{\gamma_{vw}(0)}, \quad \psi := \sum_{\ell \in \mathscr{L}} \mathbb{E}_\tau\left[I_1^\ell\right] \sum_{k=1}^{N_p} \mathbb{E}_\tau\left[I_n^k\right],$$

and

$$\kappa_m := \sum_{\substack{n=1 \\ n \neq m}}^{N_u} \kappa_{m,n}, \quad \kappa_{m,n} := \sum_{j=0}^{N_c N_f - 1} \mathscr{C}_{m,n}^{+2}(j) + \mathscr{C}_{m,n}^{-2}(j),$$

$$\xi_m := \sum_{\substack{n=1 \\ n \neq m}}^{N_u} \xi_{m,n}, \quad \xi_{m,n} := \sum_{j=0}^{N_c N_f - 1} \mathscr{C}_{m,n}^{+}(j)\mathscr{C}_{m,n}^{-}(j).$$

Expression (20) clearly shows the contribution of the impulse shape through function $\gamma_{vw}(\cdot)$, the codes through κ_1 and ξ_1 and the channel through ψ. The interesting property of this expression is that the codes contribution appears in factor of the other terms and thus can be optimized independently from the channel and the pulse shape. Based upon this property, we derive in Section IV a criterion that allows to find optimal codes for minimizing the MUI.

B. Variance of z_3 in the PAM Case

In the PAM case, the expression (13) can be re-expressed the same way as done in the Appendix for the PPM case, and takes the form:

$$\begin{aligned} y_{k,\ell,n}(\theta_n) &= d_n(-Q_n^{k,\ell} - 1)\big[\mathscr{C}_{1,n}^{-}(q_n^{k,\ell}) r_{ww}(\varepsilon_n^{k,\ell}) \\ &+ \mathscr{C}_{1,n}^{-}(q_n^{k,\ell}+1) r_{ww}(\varepsilon_n^{k,\ell} - T_c)\big] \\ &+ d_n(-Q_n^{k,\ell})\big[\mathscr{C}_{1,n}^{+}(q_n^{k,\ell}) r_{ww}(\varepsilon_n^{k,\ell}) \\ &+ \mathscr{C}_{1,n}^{+}(q_n^{k,\ell}+1) r_{ww}(\varepsilon_n^{k,\ell} - T_c)\big], \end{aligned}$$

with $r_{ww}(s) := \int_{-\infty}^{+\infty} w(u) w(u - s) du$.

Following the same derivation as for the PPM case, we find that the variance of z_3 is given by:

$$\begin{aligned}\mathbb{E}_{a,d,\theta_n}(z_3^2) &= \frac{\gamma_{ww}(0)}{N_f T_f} \sum_{\ell \in \mathscr{L}} I_1^\ell \sum_{k=1}^{N_p} \sum_{n=2}^{N_u} I_n^k \\ &\times \sum_{q=0}^{N_c N_f - 1} \big[\mathscr{C}_{1,n}^{-2}(q) + \mathscr{C}_{1,n}^{+2}(q)\big], \quad (21)\end{aligned}$$

with $\gamma_{ww}(s) := \int_{-\infty}^{+\infty} r_{ww}(u) r_{ww}(u - s) du$. Using the same definitions introduced for the PPM case, (21) can be rewritten as:

$$\sigma_3^2 = \frac{\psi\ \gamma_{ww}(0)}{N_f T_f} \kappa_1. \quad (22)$$

IV. A Criterion for Checking Time-Hopping Code Optimality

A. Notations and Preliminary Results

Let us define the following quantities:

$$\mathscr{C}_{m,n}(j) := \mathscr{C}^{+}_{m,n}(j) + \mathscr{C}^{-}_{m,n}(j), \quad (23)$$

$$S_{m,n} := \sum_{j=0}^{N_c N_f - 1} \mathscr{C}_{m,n}(j), \quad (24)$$

$$\chi_{m,n} := \sum_{j=0}^{N_c N_f - 1} \mathscr{C}^{2}_{m,n}(j). \quad (25)$$

According to (34) and (36) in the Appendix, $\mathscr{C}_{m,n}(j)$ can be interpreted as the cyclic cross-correlation between DTHC of user m and user n for a given delay j. It can be also seen as the number of collisions that occur between the impulses of signal $v_n(t)$ and $s_m(t-\tau)$ over the interval $[0, N_f T_f)$ with $jT_c \leq \tau < (j+1)T_c$. In the rest of the paper we will refer $\mathscr{C}_{m,n}(j)$ to as "collisions". Since $\mathscr{C}_{m,n}(j)$ can be seen as a cyclic cross-correlation, it can be also classically expressed using a vector notation: $\mathscr{C}_{m,n}(j) = \mathbf{c}_m^T \mathbf{Z}_j \mathbf{c}_n$, where $\mathbf{c}_i := [c_i(0), \cdots, c_i(N_c N_f - 1)]^T$ is the $(N_c N_f \times 1)$ vector composed of c_i code values, and $\mathbf{Z}_j$ is the cyclic permutation matrix obtained by k-left cyclic permutations of the columns of the $(N_c N_f \times N_c N_f)$ identity matrix $\mathbf{I}$. This matrix has a Toeplitz structure with the first column equals to $\mathbf{e}_j$ and the first line equals to $\mathbf{e}_{N_c N_f - j}$, where $\mathbf{e}_i$ is the vector with a '1' on the i-th entry and zero elsewhere. Using this vectorial notation, we can now then state the following property:

Proposition 1 $S_{m,n} = N_f^2$, $\forall m, n$.

Proof: Using the vector notation we have $S_{m,n} = \mathbf{c}_m^T \sum_{j=0}^{N_c N_f - 1} \mathbf{Z}_j \mathbf{c}_n$. Using the identity $\sum_{j=0}^{N_c N_f - 1} \mathbf{Z}_j = \mathbb{1}\mathbb{1}^T$ where $\mathbb{1}$ is the vector composed with '1' on all entries, we have $S_{m,n} = \mathbf{c}_m^T \mathbb{1}\mathbb{1}^T \mathbf{c}_n$. Since vectors $\mathbf{c}_i$ has N_f non-null entries equal to '1', we have $\mathbf{c}_m^T \mathbb{1} = \mathbf{c}_n^T \mathbb{1} = N_f$ and thus $S_{m,n} = N_f^2$. ∎

It is convenient to note that $S_{m,n}$ can be re-expressed as $S_{m,n} = \sum_{i=1}^{N_f} i \cdot \pi_i$ where $\pi_i \geq 0$ is number of times that $\mathscr{C}_{m,n}(j) = i$ occurs in the summation (24). Thus, we deduce from Proposition 1 that the π_i's should verify:

$$\sum_{i=1}^{N_f} i \cdot \pi_i = N_f^2. \quad (26)$$

Using the same argument, we can re-express (25) as:

$$\chi_{m,n} = \sum_{i=1}^{N_f} i^2 \cdot \pi_i. \quad (27)$$

B. Useful Properties

In this Section we give some properties that will be useful in section IV-C for deriving the criterion of optimality. Unless specified, we will consider in the following that $m \neq n$.

Proposition 2 $\chi_{m,n}$ *is bounded by* $N_f^2 \leq \chi_{m,n} \leq N_f^3$, $\forall m, n$.

Proof: For the lower bound, from (26) we have $\pi_1 = N_f^2 - \sum_{i=2}^{N_f} i \cdot \pi_i$, which replaced into (27) gives: $\chi_{m,n} = N_f^2 + \sum_{i=2}^{N_f} (i^2 - i) \cdot \pi_i$. Because $(i^2 - i) > 0$ for $2 \leq i \leq N_f$, we deduce that the lowest value is obtained when $\{\pi_i = 0\}_{i=2}^{N_f}$ and is then equal to N_f^2 with $\pi_1 = N_f^2$. Regarding the upper bound, we can easily check that $\chi_{m,n} = N_f^3$ is obtained when $\pi_{N_f} = N_f$ and $\pi_i = 0$ otherwise. We show now that this is the maximum value achievable. Let us assume that we have now $\pi_{N_f} = N_f - k$ where $0 < k \leq N_f$ and let us demonstrate that in that case $\chi_{m,n} < N_f^3$. From (26) we have $(N_f - 1)\pi_{N_f - 1} = N_f^2 - (N_f - k)N_f - \sum_{i=1}^{N_f - 2} i \cdot \pi_i$. Replacing this expression into (27) gives after a few computation: $\chi_{m,n} = N_f^3 - N_f k + \sum_{i=1}^{N_f - 2} i(i - N_f + 1) \cdot \pi_i$. Because $\sum_{i=1}^{N_f - 2} i(i - N_f + 1) \cdot \pi_i < 0$, we deduce that $\chi_{m,n} < N_f^3$, which concludes the proof. ∎

We have established in Proposition 2, that the minimum value of $\chi_{m,n}$ is equal to N_f^2. Now, we are going to demonstrate that when $\chi_{m,n}$ achieves its minimum value, it is equivalent to minimizing jointly ξ_m and κ_m.

Proposition 3 $\chi_{m,n} = N_f^2 \Rightarrow \mathscr{C}^{+}_{m,n}(j)\mathscr{C}^{-}_{m,n}(j) = 0 \ \forall j$.

Proof: We know from proof of Proposition 2 that codes verifying $\chi_{m,n} = N_f^2$ correspond to the case $\{\pi_i = 0\}_{i=2}^{N_f}$ and $\pi_1 = N_f^2$, from which we can deduce that the number of collisions can only be equal to 0 or 1, *i.e.*, $\mathscr{C}_{m,n}(j) \in \{0, 1\}$. This implies, because of definition (23), that when $\mathscr{C}_{m,n}(j) = 1$ then $\mathscr{C}^{-}_{m,n}(j)$ and $\mathscr{C}^{+}_{m,n}(j)$ can never be equal (one is equal to 0 whereas the other is equal to 1) and thus $\mathscr{C}^{+}_{m,n}(j)\mathscr{C}^{-}_{m,n}(j) = 0$. ∎

Proposition 4 $\kappa_{m,n} \geq N_f^2$.

Proof: From Proposition 1 we have $\sum_{j=0}^{N_c N_f - 1} \mathscr{C}^{+}_{m,n}(j) + \mathscr{C}^{-}_{m,n}(j) = N_f^2$. Then, since the partial collisions $\mathscr{C}^{+}_{m,n}(j)$ and $\mathscr{C}^{-}_{m,n}(j)$ are positive or null integers, and thanks to the identity $a^2 \geq a$ for $a \in \mathbb{N}$, we have $\sum_{j=0}^{N_c N_f - 1} \mathscr{C}^{+2}_{m,n}(j) + \mathscr{C}^{-2}_{m,n}(j) \geq N_f^2$. ∎

Proposition 5 *The minimum value for* $\xi_{m,n}$ *is* 0.

Proof: Since the partial collisions $\mathscr{C}^{+}_{m,n}(j)$ and $\mathscr{C}^{-}_{m,n}(j)$ are positive or null integers, thus $\xi_{m,n} \geq 0$. The minimum value is achieved, for instance, when $\chi_{m,n} = N_f^2$ according to Proposition 3. ∎

Lemma 1 $\chi_{m,n} = N_f^2 \Leftrightarrow \xi_{m,n}$ *is minimum* ($\xi_{m,n} = 0$) *and* $\kappa_{m,n}$ *is minimum* ($\kappa_{m,n} = N_f^2$).

Proof: For the implication, Proposition 3 shows that $\xi_{m,n} = \sum_{j=0}^{N_c N_f - 1} \mathscr{C}^{+}_{m,n}(j)\mathscr{C}^{-}_{m,n}(j) = 0$ and thus, from Proposition 5, that it reaches its minimum value. We can rewrite (25) as $\chi_{m,n} = \kappa_{m,n} + 2\xi_{m,n}$. Thus, when $\xi_{m,n} = 0$, we find that $\kappa_{m,n} = N_f^2$, which according to Proposition 4, reaches its minimum value. For the reverse, by construction, using Proposition 4 and Proposition 5, when $\kappa_{m,n} = N_f^2$ and $\xi_{m,n} = 0$ thus $\chi_{m,n} = \kappa_{m,n} + 2\xi_{m,n} = N_f^2$. ∎

TABLE I
PERCENTAGE AND NUMBER OF OPTIMAL PAIR (N_{op}) OF CODES VS. N_c

$N_f = 3$					
N_c	3	4	10	15	18
%	5.13	8.33	43.22	57.72	64.32
N_{op}	3.5×10^2	2.0×10^3	4.9×10^5	5.7×10^6	1.7×10^7
$N_f = 4$					
N_c	4	5	10	15	18
%	0.69	1.20	8.55	20.55	27.35
N_{op}	3.3×10^4	1.9×10^5	4.9×10^7	1.3×10^9	5.5×10^9

C. Criterion for Optimal Time-Hopping Codes

The optimal codes we are looking for are those which minimize the MUI variance given by (20) for the PPM or (22) for the PAM. Based upon Propositions and Lemma from the previous section, we can then state the following theorem:

Theorem 1 *Let us consider an asynchronous Time-Hopping Code Impulse Radio transmission scheme, where N_u users are transmitting through general multipath channels (as described in Section II-B). Let us consider a maximal ratio combining rake receiver, demodulating data of one of the N_u users, let say user 1. Then, the multi-user interference variance at the output of the rake receiver is minimum, if and only if, the set of pair of codes $\{(c_1, c_n),\ n = 2, \cdots, N_u\}$, verifies the conditions:*

$$\textit{for the PPM} \qquad \sum_{q=0}^{N_c N_f - 1} \mathscr{C}_{1,n}^2(q) = N_f^2, \tag{28}$$

$$\textit{for the PAM} \qquad \sum_{q=0}^{N_c N_f - 1} [\mathscr{C}_{1,n}^{-2}(q) + \mathscr{C}_{1,n}^{+2}(q)] = N_f^2, \tag{29}$$

where $\{\mathscr{C}_{1,n}(j)\}_{j=0}^{N_c N_f - 1}$ is the cyclic cross-correlation between the developed time-hopping code of user 1 and user n. A pair of codes verifying (28) or (29) is called an "optimal pair".

Proof: For the PPM, from (20), we wish to identify a criterion that we may enable us to select pairs which minimizes $\kappa_m + \bar{\gamma} \cdot \xi_m$, or equivalently, since $\bar{\gamma} \geq 0$, which jointly minimizes κ_m and ξ_m. Due to the fact that $\kappa_{m,n} \geq 0$ and $\xi_{m,n} \geq 0$, minimizing κ_m and ξ_m jointly is equivalent to minimizing for all n, $\kappa_{m,n}$ and $\xi_{m,n}$ jointly. Thus, due to the equivalence of Lemma 1, we deduce that one criterion possible is the minimization of $\chi_{m,n}$, which is equivalent to minimizing $\sum_{j=0}^{N_c N_f - 1} \mathscr{C}_{m,n}^2(j)$. For the PAM, from (22) we need to minimize the set $\{\kappa_{1,n}\}$ for $n = 2, \cdots, N_u$. Since those values are positive by definition and independent, we immmediatly deduce (29). ■

One can remark that when $\bar{\gamma} = 0$ in the PPM case, the criterion to be minimized (deduced from (20)) reduces to the PAM one. Thus, we can deduce that the set of optimal pairs for the PAM includes those of the PPM.

Notice that we have assumed equal power at the transmitter for all the users, but it is straightforward to see that the result of Theorem 1 extends to the case where all the users have different powers (it could be easily seen by including the different transmitted power in the channel model). When guard time is used, one can note that the optimal pairs may be different from those found without guard time.

Theorem 1 enables us to check if a pair is optimal or not, but it does not provide any method for constructing the optimal codes. However, for a given user n_0, it is possible, via exhaustive search, to find the set of all the optimal pairs (c_{n_0}, c_m). All the users (or nodes) belonging to this set, constitutes a network where the users can transmit at the same time while user n_0 is able to demodulate any subset, while experiencing the least MUI possible.

D. On the Selection of Optimal Code Parameters

The THC depend on two parameters: N_f and N_c. Thus, the question one may ask is how to choose those parameters, and how are they related to pair of codes optimality? In this section we open the discussion without giving any formal proof, but we give some hints based upon exhaustive search. We assume here that N_f is fixed and see what is the influence of N_c upon the code optimality. We fix N_f because it plays the role of processing gain, and is usually used in order to adjust the link budget of the transmission. Thus, N_c remains the parameter that we can adjust for a given N_f. For a given couple (N_c, N_f), the number of code is equal to $N := N_c^{N_f}$ which increases with N_c and the number of available pairs is equal to $N(N-1)/2$. When N increases, one may imagine that the number of optimal pairs increases as well. This can be verified on a few couples (N_c, N_f) and is illustrated in Table I, which shows the percentage of optimal pairs versus N_c, and the number of optimal pairs (N_{op}) obtained by exhaustive search. We can notice that the number of optimal pairs increases when N_c increases. Another result that we can deduce from Table I is that, when N_f increases, N_c should be increased too to obtain the same percentage of optimal pairs. Because the simulation complexity is exponential (see Table I), we cannot compute this percentage for large value of N_c, but we conjecture that the percentage of optimal pairs goes toward 100 % when N_c goes to infinity for a given N_f. Consequently, if we want to accommodate a given number of users, N_c should be chosen large enough to ensure that there are enough optimal codes to distribute.

Remark 1: From Proposition 3, we deduce that the maximum cross-correlation value $\mathscr{C}_{m,n}(j)$ over all the delays j, is equal to 1, which is the non-null smallest value achievable. Thus, we deduce that the optimal pairs verifying Theorem 1 for the PPM also minimize: $\sup_j \mathscr{C}_{m,n}(j)$.

Remark 2: Since the TH-IR multiple access scheme can be seen as the dual in time of the Frequency-Hopping (FH) one, some authors have proposed to use codes, introduced for FH multiple access, (such as for instance different order congruence *e.g.*, [13], or permutation sequences [14]) to TH-IR (see *e.g.*, in [15], and [16]). Using our notations, we can identify that the design of such codes is equivalent to have $N = N_c = N_f$, where N is usually the number of subcarrier. Inasmuch as this constraint is required, we deduce that this design is not suitable since it leads to the worst case (in terms of number of optimal pairs) as shown in Table I.

Remark 3: The computation of the MUI variance has been tackled by other authors. The earlier work can be found in [2]

for free-space propagation and has been extended to multipath channels in [6]. The difference between those works and our is that they rely upon different hypothesis. The main difference is the random assumption for the asynchronism, which they assume to be equally likely distributed (*eld*) over $[0, T_f)$, whereas we assume that it is *eld* over $[0, N_f T_f)$. We think our assumption is more appropriate since the code period is spread over $[0, N_f T_f)$ which implies that the signal is cyclo-periodic with period $N_f T_f$. Thus, if we want to account for any asynchronism, *i.e.*, $\theta_n \in [0, +\infty)$, it is equivalent to consider its restriction to $[0, N_f T_f)$. The other difference is that they assume $N_c T_c < T_f/2 - 2T_w$ (*e.g.,* see Eq. (57) in [8]) which corresponds to a guard time of more than $50\ \%$ of the frame duration. As a consequence, this allows to approximate the MUI variance expression by neglecting some terms, which in the end does not depend upon the codes. This explains that, even if they assume the THC as discrete random variables, uniformly distributed, they never compute the expectation over the codes in their derivations. The codes could have been chosen as deterministic, the results would have been the same. Although they consider the case $N_f \geq 1$, their approach corresponds to our as if $N_f = 1$. In that case, the collisions are at most equal to 1, and thus all the pairs are optimal.

V. Performance Analysis

In this section, we study the influence of the optimality of pair of codes on the Average Error Probability (AEP) at the rake receiver. We check by simulations that the optimal pairs (pair of codes minimizing the MUI variance) enable us to decrease the AEP significantly. After explaining how the AEP is computed, we give the simulation parameters and then define the different tested configurations.

A. Average Error Probability Computation

For a given set of random parameters (channel amplitudes, channel delays, symbols, asynchronism, and noise), the error probability at the rake output (11), is given by $P_e(a, \tau, d, \theta, n) = \Pr\{z < 0 | a, \tau, d, \theta, n\}$, assuming that $d_1(0)$, the transmitted symbol of the user of interest, is fixed ($d_1(0) = 0$ for the PPM, and $d_1(0) = 1$ for the PAM). The AEP is then obtained by averaging $P_e(a, \tau, d, \theta, n)$ using empirical mean over all the random variables. Rather than doing that, we can reduce the simulation complexity by taking advantage of the fact that the noise is Gaussian. In that case, the AEP is given by $\bar{P}_e = \mathbb{E}_{a,\tau,d^*,\theta^*}[\Pr\{z < 0 | a, \tau, d, \theta\}]$ with $d^* = d \setminus \{d_1(0)\}$ and $\theta^* = \theta \setminus \{\theta_1\}$. Since the noise is Gaussian with zero mean and using (14), we have:

$$\bar{P}_e = \mathbb{E}_{a,\tau,d^*,\theta^*}\left[\frac{1}{2}\mathrm{erfc}\left(\frac{z_1 + z_2 + z_3}{\sqrt{2}\,\sigma_\eta}\right)\right], \qquad (30)$$

where σ_η^2 is the variance of the filtered Gaussian noise.

Thus, there is no need for simulating the noise. Notice that this approach have been used in [10] in the same context but in the free-space propagation setting. It is interesting to point out that in our case, the noise variance σ_η^2 is not a constant and depends upon the channel realization.

By considering that optimizing the MUI variance with respect to the THC is a relevant task, we have implicitly assumed that the MUI is Gaussian (as in [8] for instance). Unfortunately as observed in [9], the MUI is not Gaussian and the AEP given by (30) is actually much larger that the error probability computed under the Gaussian MUI assumption. According to intensive simulations, we will see hereafter that the codes optimization based on the minimization of the MUI variance remains valid in practice, *i.e.*, the AEP for optimized codes (chosen implicitly under Gaussian assumption) is much smaller than those of non-optimized ones.

B. Simulation Parameters and Scenario Description

We give here the different simulation parameters that will be used for computing the performance. Remembering that we want to assess the effect of optimality of pairs on performance, it is worth noting that, since the channel, rake, and pulse parameters appear in factor of the MUI variance, their choice is not critical. Therefore, whatever the set of parameters we choose, we show the same trends regarding the optimality. We have considered the CM2 channel model from the TG3a [11], with one cluster for simplicity. The number of finger is fixed to $L_r = 3$, and the number of paths N_p, is chosen such that the average energy of the amplitude drops below $1/100$ of its maximum value (set to 1), *i.e.*, $\exp\{\gamma^{-1}\tau_1^{N_p}\} \leq 100$, which according to $\gamma = 6.7$ ns in CM2, gives $\tau_1^{N_p} \leq 30.85$ ns. We have considered a modulated Gaussian pulse such that its power spectral density fits the outdoor FCC mask [3], in the $[3.1\,\mathrm{GHz} - 10.6\,\mathrm{GHz}]$ band. This is achieved by translating the Gaussian baseband spectrum to the central frequency of the mask *i.e.*, $f_0 = 6.85$ GHz. Then, the width of the pulse is adjusted to fit the mask, *i.e.*, to have the required 20 dB attenuation at both side of the mask. For practical purpose, the pulse is truncated to duration $T_w = 1$ ns, and thus, can be written as:

$$w(t) = \sqrt{\frac{2}{\pi}}\cos(2\pi f_0(t - T_w/2))e^{-(t-T_w/2)^2/2\sigma^2} \times \mathbb{1}_{[0,T_w]},$$

with $\sigma^2 = 911 \times 10^{-4}$ ns. For the PPM, the delay is set to $\delta = 0.0707$ ns. The frame duration is fixed to $T_f = 60$ ns and the chip duration is given by $T_c = T_f/(N_c + N_g)$, with N_g the number of chips dedicated to the guard interval. Consequently, the symbol rate is equal to $(N_f T_f)^{-1}$ regardless of the guard time duration.

The number of users is fixed at $N_u = 7$, and the user of interest is user 1. To check the benefit of our code optimization procedure, we inspect the AEP for three different scenarios, namely A, B, and C. For each scenario, we fix the THC of user 1 (c_1) and select three different sets of six codes $\{c_i, i = 2, \cdots, 7\}$. Those sets will be referred to as $0/6$, $3/6$, and $6/6$, which correspond to zero, three, and six optimal pairs with respect to user 1.

Scenario A: shows the maximum gain in performance that can be achieved using optimal pairs. For that, we fix c_1 such that the non-optimal pairs yield the maximal MUI variance. This corresponds, according to Proposition 2, to codes verifying $\chi_{1,n} = N_f^3 = 27$, which are given by $\tilde{c}_1 = \{0, 0, 0\}$, and $\tilde{c}_n = \{n-1, n-1, n-1\}$ for $n = 2, \cdots, N_c - 1$. The modulation format is PPM.

Scenario B: shows that, even when the code of user 1 is chosen at random (not the worst case as in scenario A), we can

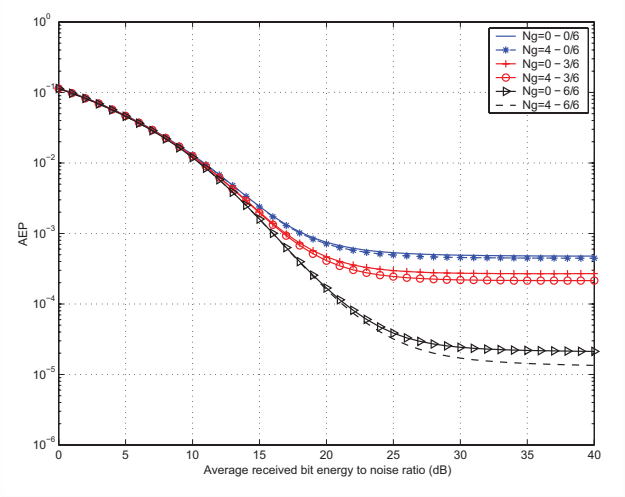

Fig. 1. Average error probability vs. $\bar{E}_b/N_0$ for scenario A, with PPM format, SRAKE receiver with $L_r = 3$ fingers, $N_u = 7$, $N_f = 3$, and $N_c = 18$. With guard time, $N_g = 4$, and without, $N_g = 0$.

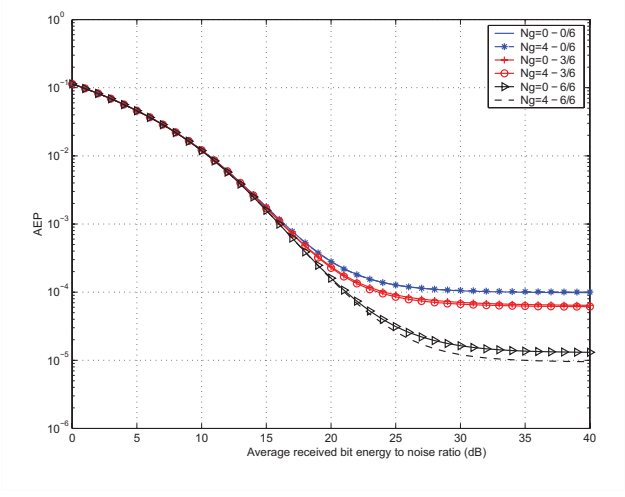

Fig. 2. Average error probability vs. $\bar{E}_b/N_0$ for scenario B, with PPM format, SRAKE receiver with $L_r = 3$ fingers, $N_u = 7$, $N_f = 3$, and $N_c = 18$. With guard time, $N_g = 4$, and without, $N_g = 0$.

still find optimal pairs that lead to performance improvement. Noting that in scenario A we have $\chi_{1,1} = \chi_{1,n}$, we decide to choose the non-optimal codes likewise. Code of user 1 has been picked up equal to $\tilde{c}_1 = \{0, 0, 2\}$ which correspond to $\chi_{1,1} = 15$. The modulation format is PPM.

Scenario C: same scenario as scenario B, with PAM format.

For all scenarios, we have also selected optimal pairs and computed performance when a guard time is used, with $N_g = 4$.

C. Performance Analysis

The simulations have been carried out by averaging the error probability (30) using 10^6 random trials. The results shown in Fig. 1 to Fig. 3 represent the AEP versus the average received bit energy to noise ratio, $\bar{E}_b/N_0$, with $\bar{E}_b = \mathbb{E}_{a,\tau,d,\theta}\{\int_0^{N_f T_f} r_1^2(t)dt\}$. For the TG3a channel model (with one cluster), we find $\bar{E}_b = N_f r_{ww}(0) \cdot \sum_{k=1}^{N_p} \mathbb{E}_\tau(I_1^k)$ with $\mathbb{E}_\tau(I_1^k) = \lambda^k(\lambda + 1/\gamma)^{-k}$. For scenario A, results in Fig. 1

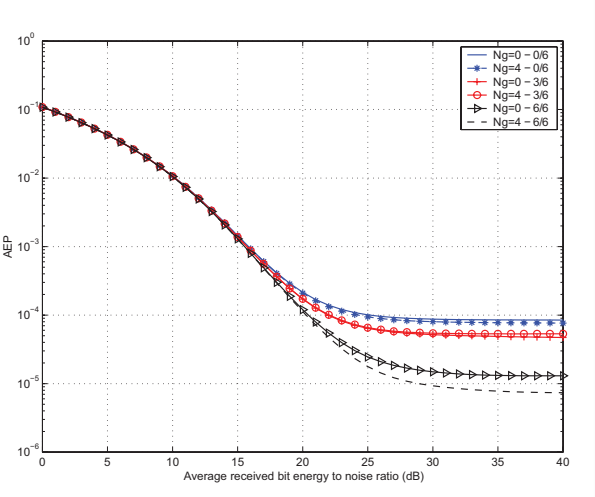

Fig. 3. Average error probability vs. $\bar{E}_b/N_0$ for scenario C, with PAM format, SRAKE receiver with $L_r = 3$ fingers, $N_u = 7$, $N_f = 3$, and $N_c = 18$. With guard time, $N_g = 4$, and without, $N_g = 0$.

show that the performance increases as the number of optimal pairs increases as expected. For high $\bar{E}_b/N_0$, the gain in performance between the best and the worst case is around 22. For scenario B, we see in Fig. 2 that the behavior is the same as for scenario A, but the gain in performance is smaller (around 7.5). This gain was predictable since the set $0/6$ does not represent the worst case as in scenario A. For scenario C, Fig. 3 shows that the PAM behaves like the PPM with respect to the different set. The gain in performance is a little bit smaller (around 6.5). This can be explained by the fact that the MUI variance in the non-optimal case is greater for the PPM case than for the PAM one (see (20) and (22)).

For the three scenarios, we can see that with guard time, the performance behavior is similar to the case without guard time, *i.e.*, when the number of optimal pairs increases, the performance increases. One can note that the performance improvement with guard time is not significant. This can be explained by the fact that the maximum delay of the channel is actually less than the frame duration, and thus, there is no ISI. This was done on purpose in order to isolate the effect of MUI optimization from the effect of the ISI. Nevertheless, the fact that the performance is slightly different illustrates the limit of the Gaussian approximation, *i.e.*, although the MUI variance is equal in both cases, the AEP are different.

VI. Conclusion

A criterion that allows to check code optimality that minimizes the MUI variance at the output of a rake receiver has been proposed. The result has been derived by computing the exact variance expression of the MUI considering that the codes are deterministic. For very general assumptions on the channel and the rake receiver, the expression of the MUI variance, shows that the code contribution appears in factor and is independent of the other parameters of the transmission scheme. We have deduced from this expression a practical criterion that allows to select a set of optimal codes that ensures minimal MUI variance at the output of the rake receiver. This

criterion involves partial cyclic cross-correlation of the DTHC. Simulations have shown that minimizing the MUI variance (based on a SNR criterion) leads to a significant decrease of the error probability. Thus, the proposed criterion appears as a useful tool for designing THC in IR-THC transmissions. Further work will be needed in order to find algorithms for constructing optimal pair of codes without exhaustive search.

APPENDIX

COMPUTATION OF TERMS $y_{k,\ell,n}(\theta_n)$ VERSUS DTHC IN THE PPM CASE

We present in this Appendix the computation of terms $y_{k,\ell,n}(\theta_n)$ defined by (12) in the PPM case which correspond to the cross-correlation of the k-th path of the incoming signal from user n with the template signal synchronized on the ℓ-th path of user 1. Assuming θ_n fixed, we put:

$$\theta_n + \Delta\tau_{k,\ell,n} := Q_n^{k,\ell} N_f T_f + q_n^{k,\ell} T_c + \varepsilon_n^{k,\ell}, \qquad (31)$$

with $Q_n^{k,\ell} = \lfloor (\theta_n + \Delta\tau_{k,\ell,n})/N_f T_f \rfloor$, $q_n^{k,\ell} = \lfloor (\theta_n + \Delta\tau_{k,\ell,n} - Q_n^{k,\ell} N_f T_f)/T_c \rfloor$, and $\varepsilon_n^{k,\ell} \in [0, T_c)$. Although not written for the sake of notation clarity, it is worth noting that $Q_n^{k,\ell}$, $q_n^{k,\ell}$ and $\varepsilon_n^{k,\ell}$ depend on θ_n and $\Delta\tau_{k,\ell,n}$.

Thanks to the DTHC we can isolate the non-null terms of (12), and using the following notation $r_{vw}(x) := \int_{-\infty}^{+\infty} v(t)w(t-x)dt$ we can write:

$$y_{k,\ell,n}(\theta_n) = \sum_{i=-\infty}^{+\infty} \sum_{j,j_1=0}^{N_c N_f - 1} c_n(j) c_1(j_1) \times r_{vw}((Q_n^{k,\ell} + i) N_f T_f + (q_n^{k,\ell} + j - j_1) T_c + \varepsilon_n^{k,\ell} + \delta d_n(i)). \qquad (32)$$

Let $T_{r_{vw}}$ denotes the support of function $r_{vw}(\cdot)$ is less than T_c, the non-null terms in (32) are obtained when $|\varepsilon_n^{k,\ell} + (q_n^{k,\ell} + j - j_1)T_c + (Q_n^{k,\ell} + i)N_f T_f + \delta d_n(i)| < T_{r_{vw}}$. As we have $-N_c N_f + 1 \le q_n^{k,\ell} + j - j_1 \le 2N_c N_f - 2$, the non-null terms in (32) are obtained for $-2 < Q_n^{k,\ell} + i < 1$ thus $Q_n^{k,\ell} + i$ is equal to 0 or -1.

We put now $y_{k,\ell,n}(\theta_n) := y^-_{k,\ell,n}(\theta_n) + y^+_{k,\ell,n}(\theta_n)$ where $y^-_{k,\ell,n}(\theta_n)$ corresponds to $i = -Q_n^{k,\ell} - 1$, and $y^+_{k,\ell,n}(\theta_n)$ corresponds to $i = -Q_n^{k,\ell}$.

When $i = -Q_n^{k,\ell} - 1$, we have $j - j_1 + q_n^{k,\ell} - N_c N_f = 0$ or -1, thus we can write:

$$\begin{aligned} y^-_{k,\ell,n}(\theta_n) = {} & \mathscr{C}^-_{1,n}(q_n^{k,\ell}) r_{vw}(\varepsilon_n^{k,\ell} + \delta d_n(-Q_n^{k,\ell} - 1)) \\ & + \mathscr{C}^-_{1,n}(q_n^{k,\ell} + 1) r_{vw}(\varepsilon_n^{k,\ell} - T_c + \delta d_n(-Q_n^{k,\ell} - 1)), \end{aligned} \qquad (33)$$

where:

$$\mathscr{C}^-_{1,n}(q) := \sum_{m=0}^{q-1} c_1(m) c_n(m-q). \qquad (34)$$

When $i = -Q_n^{k,\ell}$, we have $j - j_1 + q_n^{k,\ell} = 0$ or -1, thus we can write:

$$\begin{aligned} y^+_{k,\ell,n}(\theta_n) = {} & \mathscr{C}^+_{1,n}(q_n^{k,\ell}) r_{vw}(\varepsilon_n^{k,\ell} + \delta d_n(-Q_n^{k,\ell})) \\ & + \mathscr{C}^+_{1,n}(q_n^{k,\ell} + 1) r_{vw}(\varepsilon_n^{k,\ell} - T_c + \delta d_n(-Q_n^{k,\ell})), \end{aligned} \qquad (35)$$

where:

$$\mathscr{C}^+_{1,n}(q) := \sum_{m=q}^{N_c N_f - 1} c_1(m) c_n(m-q). \qquad (36)$$

We can remark that the two terms of (33) and (35) are never non-null at the same time, because the support of $r_{vw}(\cdot)$ is less than T_c. Finally we end up with the following expression:

$$\begin{aligned} y_{k,\ell,n}(\theta_n) = {} & \mathscr{C}^-_{1,n}(q_n^{k,\ell}) r_{vw}(\varepsilon_n^{k,\ell} + \delta d_n(-Q_n^{k,\ell} - 1)) \\ & + \mathscr{C}^-_{1,n}(q_n^{k,\ell} + 1) r_{vw}(\varepsilon_n^{k,\ell} - T_c + \delta d_n(-Q_n^{k,\ell} - 1)) \\ & + \mathscr{C}^+_{1,n}(q_n^{k,\ell}) r_{vw}(\varepsilon_n^{k,\ell} + \delta d_n(-Q_n^{k,\ell})) \\ & + \mathscr{C}^+_{1,n}(q_n^{k,\ell} + 1) r_{vw}(\varepsilon_n^{k,\ell} - T_c + \delta d_n(-Q_n^{k,\ell})). \end{aligned} \qquad (37)$$

REFERENCES

[1] P. II. Withington, and L. W. Fullerton, "An impulse radio communications system," in *Proc. Int. Conf. on Ultra-Wide Band, Short-Pulse Electromagnetics*, Oct. 1992, pp. 113-120.

[2] R. A. Scholtz, "Multiple access with time-hopping impulse radio," in *Proc. Milcom Conf.*, Oct. 1993, pp. 447-450.

[3] Federal Communication Commission, "Revision of Part 15 of the commission's rules regarding ultra-wideband transmission systems, first report and order," FCC, Feb. 2002.

[4] IEEE 802.15.3a WPAN High Rate Alternative PHY Task Group 3a (TG3a). [Online] Available: http://www.ieee802.org/15/pub/TG3a.html

[5] C. J. Le Martret and G. B. Giannakis, "All-Digital impulse radio for wireless cellular systems," *IEEE Trans. Commun.*, vol. 50, no. 9, pp. 1440-1450, Sep. 2002.

[6] F. Ramírez-Mireles, "Error probability of ultra wideband SSMA in a dense multipath environment," in *Proc. Milcom Conf.*, Oct. 2002, vol. 2, pp. 1081-1084.

[7] A. A. M. Saleh, and R.A. Valenzuela, "A statistical model for indoor multipath propagation," *IEEE J. Select. Areas Commun.*, vol. 5, no. 2 pp. 128-137, Feb. 1987.

[8] M. Z. Win and R. A. Scholtz, "Ultra-wide bandwith time-hopping spread-spectrum impulse radio for wireless multiple-access communications," *IEEE Trans. Commun.*, vol. 48, no. 4, pp. 679-691, Apr. 2000.

[9] G. Durisi and G. Romano, "On the validity of Gaussian approximation to characterize the multiuser capacity of UWB TH-PPM," in *Digest of Papers-IEEE Conference on Ultra Wideband Systems and Technologies*, May 2002, pp. 157-162.

[10] G. Durisi and S. Benedetto, "Performance evaluation of TH-PPM UWB systems in the presence of multiuser interference," *IEEE Commun. Lett.*, vol. 7, no. 5, pp. 224-226, May 2003.

[11] A. F. Molish, J. R. Foerster, and M. Pendergrass, "Channel models for ultrawideband personal area networks," *IEEE Wireless Commun. Mag.*, vol. 10, no. 6, Dec. 2003.

[12] A. Rajeswaran, V. Srinivasa Somayazulu, and J. R. Foerster, "Rake performance for a pulse based UWB system in a realistic UWB indoor channel," in *Proc. IEEE International Conference on Communications*, May 2003, no. 1, pp. 2879-2883.

[13] S. V. Marić and E. L. Titlebaum, "Frequency hop multiple access codes based upon the theory of cubic congruences," *IEEE Trans. Aerosp. Electron. Syst.*, vol. 26, no. 6, pp. 1035-1039, Nov. 1990

[14] O. Moreno and S.V. Marić, "A new family of frequency hop codes," *IEEE Trans. Commun.*, vol. 48, no. 8, pp. 1241-1244, Aug. 2000

[15] T. Erseghe, "Ultra Wide Band Pulse Communications." Ph. D. thesis, Universitá degli Studi di Padova, 2001.

[16] R. A. Scholtz, P. V. Kumar, and C. J. Corrada-Bravo, "Signal Design for Ultra-wideband Radio," *Sequences and Their Applications-Proceedings of SETA'01*, T. Helleseth, P. V. Kumar, and K. Yang, eds. Springer-Verlag France, 2002.

Christophe Le Martret was born in Rennes, France, on March 12, 1963. He received the Ph.D. degree in Signal Processing and Communications from l'Université de Rennes 1, Rennes, France, in 1990. From 1991 to 1995 he was with the CESTA, Bruz, France, and from 1996 to 2002 with the Centre d'Électronique de L'ARmement (CELAR). In 2002 he joined the Signal Processing and Multimedia Department at Thales Communications France. He was a Visiting Researcher at the SpinCom Laboratory, Department of ECE, University of Minnesota, MN, USA, from 1999 to 2000. He currently works as an R&D Program Manager in the field of radio access for wireless communications including cross-layers optimization, ultra wideband (UWB), multi-user detection, and cognitive radio.

Anne-Laure Deleuze was born in Marseille, France in 1978. She received the Master Science degree in digital communications from Ecole Nationale Supérieure des Télécommunications (ENST) de Paris, France in 2002. She is currently working with THALES Land and Joint Systems, Colombes, France toward the Ph.D. degree from ENST. Her current research is devoted to multi-user UWB communication systems, UWB channel estimation, and low-complexity receiver design.

Philippe Ciblat was born in Paris, France, in 1973. He received the Engineer degree from the Ecole Nationale Supérieure des Télécommunications (ENST) and the DEA degree (french equivalent to M.Sc.) in Automatic Control and Signal Processing from the University of Orsay, both in 1996. He also received the Ph.D. degree from Laboratoire Système de Communication of the University of Marne-la-Vallée in 2000. His Ph.D. thesis focused on estimation issue (blind equalization and frequency synchronization) in non-cooperative telecommunications. In 2001, he held a postdoctoral researcher position with the Laboratoire des Télécommunications, Université catholique de Louvain, Belgium. At the end of 2001, he joined as Associate professor the department of Communications and Electronics at ENST. His research areas include statistical and digital signal processing (blind equalization, frequency estimation, and asymptotic performance analysis), and signal processing for digital communications (synchronisation for OFDM modulations and CDMA scheme, acces technique and localization for UWB, design of global wireless systems).

Since 2004, he also serves as Associate Editor for IEEE COMMUNICATIONS LETTERS. He is involved in a few industrial projects with THALES Land and Joint Systems and Sagem.